EINDHOVEN UNIVERSITY OF TECHNOLOGY

Guidelines for external fixation frame rigidity and stresses

Citation for published version (APA):
Huiskes, H. W. J., & Chao, E. Y. S. (1986). Guidelines for external fixation frame rigidity and stresses. *Journal of Orthopaedic Research*, *4*(1), 68-75. https://doi.org/10.1002/jor.1100040108

DOI:
10.1002/jor.1100040108

Document status and date:
Published: 01/01/1986

Document Version:
Publisher's PDF, also known as Version of Record (includes final page, issue and volume numbers)

Please check the document version of this publication:

• A submitted manuscript is the version of the article upon submission and before peer-review. There can be important differences between the submitted version and the official published version of record. People interested in the research are advised to contact the author for the final version of the publication, or visit the DOI to the publisher's website.
• The final author version and the galley proof are versions of the publication after peer review.
• The final published version features the final layout of the paper including the volume, issue and page numbers.

Link to publication

General rights
Copyright and moral rights for the publications made accessible in the public portal are retained by the authors and/or other copyright owners and it is a condition of accessing publications that users recognise and abide by the legal requirements associated with these rights.

• Users may download and print one copy of any publication from the public portal for the purpose of private study or research.
• You may not further distribute the material or use it for any profit-making activity or commercial gain
• You may freely distribute the URL identifying the publication in the public portal.

If the publication is distributed under the terms of Article 25fa of the Dutch Copyright Act, indicated by the "Taverne" license above, please follow below link for the End User Agreement:

www.tue.nl/taverne

Take down policy
If you believe that this document breaches copyright please contact us at:

openaccess@tue.nl

providing details and we will investigate your claim.

Download date: 16. Nov. 2023

Journal of Orthopaedic Research
4:68–75, Raven Press, New York
© 1986 Orthopaedic Research Society

Guidelines for External Fixation Frame Rigidity and Stresses

R. Huiskes and *E. Y. S. Chao

*Laboratory for Experimental Orthopaedics, University of Nijmegen, Nijmegen, The Netherlands; and *Orthopedic Biomechanics Laboratory, Mayo Clinic/Mayo Foundation, Rochester, Minnesota, U.S.A.*

Summary: Using results from FEM analyses and experiments as references, analytical methods are applied to develop simple approximate formulas to relate frame rigidity, maximal pin stresses, and peak pin–bone stresses in external fracture fixation (EFF) configurations in axial loading to the most important frame, pin, and bone parameters. It is found that, in a realistic range, the parameters can be adapted to vary the frame rigidity from about 13 N/mm to 17,000 N/mm, thereby reducing the maximal stresses in the pins and at the pin–bone interface by a factor of 140. In particular, when compromises have to be established in the frame characteristics in order to ensure a flexible configuration and limit the stress values at the same time, the formulas presented can provide useful guidelines. The side-bar separation and the pin modulus, in particular, can be adapted to decrease the rigidity, while only moderately increasing the stresses, thereby reducing chances for pin failure, pin–bone loosening, and pin-tract infection. A nomogram is presented for a quick reference to estimated relations between frame characteristics, rigidity, and stresses. It is believed that this material may be of use in EFF design and applications in clinical and animal experimental trials. **Key Words:** External fracture fixation —Biomechanics—Fracture healing.

Mechanical fixation of bone fractures by an external approach using percutaneous pins has a long history (13,14). After becoming popular in the United States during the Second World War, the enthusiasm for using such a device diminished due to the high incidence of complications (8). In the wake of recent advances in bioengineering, a renewed interest has developed regarding the design and application of these devices. Now, the application of external fixation encompasses a wide spectrum of clinical problems, including the treatment of closed fractures.

Address correspondence and reprint requests to Dr. R. Huiskes at Laboratory of Experimental Orthopaedics, University of Nijmegen, 6500 HB Nijmegen, The Netherlands.

Presented in part at the 4th General Meeting, European Society of Biomechanics, Davos, Switzerland, September 24–26, 1984.

The nature of the device lends itself ideally for bone fracture management because of the wide range of rigidities available among different frame configurations and the adjustability of their mechanical properties at any time during the course of treatment (9,11). Existing knowledge of bone fracture repair has helped to validate the potential of achieving bone fracture union under external fixation. Rigid fixation can minimize pin-tract infections secondary to loosening, while bone fracture union may follow a pattern somewhat similar to that observed in contact healing (6,10). Elastic fixation, on the other hand, usually induces more periosteal callus formation, which probably accelerates the bone fracture healing process (3).

It follows directly from this information that the ideal external fixator can provide rigidity in a wide range, from very flexible to very rigid, while at all times having adequate pin and frame strength and stable, strong connections at the pin–bone interfaces. A number of authors have addressed these requirements, using experimental and analytical methods to assess frame rigidity, pin stresses and pin–bone interface stresses for varying frame configurations and dimensions (1,2,4,5,7,9,11,12). The purpose of the present paper is not to provide additional data in this respect, but to encompass previous findings in a simple analytical model. In this model, consisting of a number of relatively simple formulas, the most important bone and frame parameters are related to the rigidity of the external fixator, the maximal pin stresses, and the maximal pin–bone interface stresses in axial loading. This model can be used to provide rough approximate guidelines for external fixation frame (EFF) design and applications in clinical trials and animal experimental work, regarding aspects of both rigidity and strength.

EFF FRAME RIGIDITY

A bilateral, full-pin EFF configuration is schematically shown in Fig. 1A. The parameters taken into account are indicated and further defined in Table 1. Also shown in Table 1 are the parameter values used to form the reference case, the basis for parametric analyses. The rigidity of the frame in axial loading is defined as $k_f = F/\Delta$ (N/mm), its flexibility as $1/k_f$ (mm/N).

It is obvious from a mechanical point of view that each pin in the fixator behaves in accordance with linear elastic beam theory, as long as the stresses do not pass the elastic (yield) limit. The internal, cross-sectional bending moment and the transverse force in a pin are denoted by $M(x)$ and $T(x)$, respectively. At the pin–bone fixation site ($x = 0$), the symbols $M(0) = M_o$ and $T(0) = T_o$ are used (Fig. 1B).

It is assumed that the axial flexibilities of the bone and the side bar are negligible relative to the axial and bending flexibilities of the pin, i.e., that they behave as rigid elements in which the pins are rigidly fixed. Therefore (Fig. 1B),

$$u(0) = \frac{\Delta}{2}, \quad u(s) = 0, \quad \left(\frac{du}{dx}\right)_0 = \left(\frac{du}{dx}\right)_s = 0 \quad (1)$$

From these boundary conditions and the differen-

1A,B

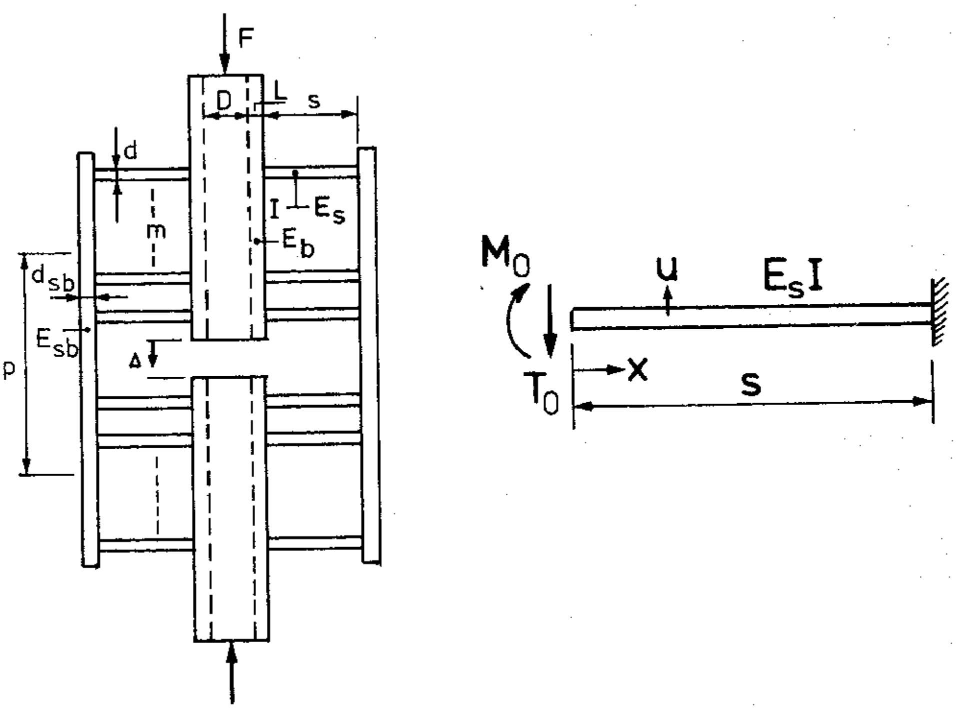

FIG. 1. Schematic bilateral EFF frame configuration **(A)** and loading configuration in a pin at the bone side **(B)**. Various parameters and variables are indicated.

tial equations for linear elastic beam theory, it is easily established that in each pin

$$M_o = (s/2)T_o \qquad (2)$$

and

$$u(0) = \frac{\Delta}{2} = \frac{s^2}{6E_sI}(2T_os - 3M_o). \qquad (3)$$

These equations are valid for each pin separately, under the assumed conditions. If all pins carry the same load, we have

$$T_o = F/n_fm \qquad (4)$$

Combining Eqs. 2–4 yields an analytical expression for the EFF frame rigidity ($k_f = F/\Delta$)

$$k_f = 6\,(n_fmE_sI/s^3) \qquad (5)$$

where $I = (\pi/64)d^4$.

Although this model is simple, its predictions compare well with more sophisticated finite element analyses and experimental results (Table 2), except, in one case, for the unilateral, half-frame configuration, the cause for which is discussed later. The experimentally determined rigidities are somewhat lower than those predicted in the FE analyses and with the present model, most likely because of flexibility in the pin connections to bone and side bar. According to the present model, the ratio M_o/T_o should be equal to $s/2$ (Eq. 2), which is also found in the FE models.

To explain the discrepancies in the frame rigidity between FE results (5) and present findings for the unilateral, half-frame configuration (Table 2), the FE analysis reported by Chao et al. (5) was repeated. It was found that in this case the bending flexibility of the side bar cannot be neglected, due to the nonsymmetry of the configuration. Taking this into account, again using beam theory, yields

$$k_f \approx \left(\frac{s^3}{6mE_sI} + \frac{s^2l_p}{E_{sb}I_{sb}}\right)^{-1} \qquad (5A)$$

where E_{sb} and I_{sb} are the modulus and area moment of the side bar, respectively, and l_p is the effective pin separation between the static gravity centers of the pin configurations on each side of the fracture. For a symmetric pin configuration, these centers are located halfway between the outer pins. The second term in the denominator of Eq. 5A accounts for the axial deflection of the bone parts due to bending deflection of the side bar. For the reference case, Eq. 5A gives $k_f = 46$ N/mm, whereas Eq. 5 gives $k_f = 170$ N/mm, which explains the FE results in Table 2. Hence, if $n_f = 1$, Eq. 5A must be used instead of Eq. 5, unless the term $s^2l_p/E_{sb}I_{sb}$ becomes negligible, which is approximately the case when the side-bar diameter is more than five times the pin diameter. An example of such a rigid side-bar configuration was studied experimentally (15). Evidently, a good agreement between the experimental results and Eq. 5 can be established in this case (Table 2). Tencer et al. (12) found much lower values for axial stiffness in their experiments with unilateral frames. This may be a result of side-bar bending, as explained above, but also of deformation in the side-bar clamps.

TABLE 1. *Definitions of symbols used for the various parameters and their values in the reference configuration*

Parameter/variable	Symbol	Unit	Reference value
Axial bone force	F	N	445
Intramedullar width	D	mm	16
Cortical thickness	L	mm	4.8
Side-bar separation	s	mm	63.5
No. of pins/fracture side	m	—	3
No. of side bars	n_f	—	2
EFF frame rigidity	k_f	N/mm	Variable
Maximal pin–bone stress	$\bar{\sigma}_{bm}$	Mpa	Variable
Bone modulus	E_b	MPa	1.52×10^4
Pin modulus	E_s	MPa	2.00×10^5
Pin diameter	d	mm	3.96
Pin area moment	I	mm^4	12.1
Foundation modulus	k	MPa	8.82×10^4
Fracture deformation	Δ	mm	Variable
EFF frame flexibility	$1/k_f$	mm/N	Variable
Maximal pin stress	σ_{sm}	MPa	Variable
Side-bar modulus	E_{sb}	MPa	2.00×10^5
Side-bar diameter	d_{sb}	mm	8.0
Side-bar area moment	I_{sb}	mm^4	201
Effective pin separation	l_p	mm	156

PIN STRESSES

The maximal pin bending stresses occur at the clamped sides, as was also found in FEM investigations (4,5). From the definition of the maximal bending stress at the bone connection side,

$$\sigma_{sm} = M_od/2I \qquad (6)$$

it follows, using Eq. 4, that

$$\sigma_{sm} = (sd/4n_fmI)F \qquad (7)$$

TABLE 2. *EFF frame rigidity values established with the present model compared with results from previous experimental and FEM analyses for several frame configurations and ratio between pin bending moment and transverse force (M_o/T_o)*

Configuration	Ref.	Experiment k_f (N/mm)	FEM-beam model k_f (N/mm)	FEM-beam model M_o/T_o	Present model k_f (N/mm)	Present model M_o/T_o
Bilateral (FP)	5	310	361	32	340	32
Unilateral (HP)	5	—	57	30–32	170/46[c]	32
Unilateral (HP)[a]	15	294/217	—	—	332/215	—
Triangular (HP + FP)	5	—	485	32	510	32
Bilateral (FP)[b]	1	65	83	—	79	53

[a] s = 28.6 mm; d = 4 mm; M = 3 pins/2 pins, respectively. All other parameters as in the reference case (Table 1).
[b] s = 107 mm; d = 4.06 mm; $E_s = 2.03 \times 10^5$ MPa. All other parameters as in the reference case.
[c] After correction for side-bar bending.

Comparing results obtained with Eq. 7 to those from FEM analyses (5) again gives good agreement, as shown in Table 3. The assumption of equal loads in all pins is also quite reasonably fulfilled in the FEM results, although the differences between pins in the unilateral configuration are significantly larger than in the other configurations. It must be noted that considerable axial pin forces are evident in the FEM model, in particular, the unilateral one, that are not considered in the analytical model. These loads do not interfere with the rigidity of the frame, but do increase the maximal pin stresses, on the order of 10% for the unilateral frame and on the order of 3% in the bilateral and triangular frames.

The effective pin diameter plays an important role in both the evaluation of maximal pin stresses and frame rigidity. For cases in which pins are threaded, the effective core diameter is reduced, while the threaded part is not fully buried within the bone; pin stresses will therefore be higher and the frame rigidity lower (12).

PIN–BONE INTERFACE STRESSES

Pin–bone interface stresses were investigated using three-dimensional and axisymmetric FEM models (4,7). From the results of these analyses, closed-form solutions based on beam-on-elastic-foundation theory were derived (7). Examples of the stress distributions obtained are shown in Fig. 2. Introducing further simplifications, a rough approximative formula was developed for the peak compressive stress ($\bar{\sigma}_{bm}$) at the pin–bone interface (7):

$$\bar{\sigma}_{bm} \approx T_o s/d\left(\frac{8E_sI}{LDk} + \frac{L^2}{3}\right) \quad (d \geq 3 \text{ mm}) \qquad (8)$$

TABLE 3. *Maximal pin bending stresses σ_{sm} established with the present model compared with results from previous FEM analyses (5)*

Parameter	Value	Maximum pin bending stress, σ_{sm} (MPa): FEM model (average over all pins)	Present model
Pin diameter d (mm)	3	866	888
	3.96	371	385
	5	191	192
No. pins m	2	556	577
	3	371	385
	4	292	289
Side-bar separation s (mm)	50	299	303
	63.5	371	385
	75	446	455
		Range in all pins	
Configuration	Unilateral	699–806	770
	Bilateral	369–372	385
	Triangular	266–272	257

Effects of variations in pin diameter, number of pins, and side-bar separation are shown, as are the ranges in the stresses of the three pins, as calculated in the FEM models (5).

Using Eq. 4, this formula transforms into

$$\bar{\sigma}_{bm} \approx \left[s/n_f m d \left(\frac{8E_s I}{LDk} + \frac{L^2}{3} \right) \right] F \quad (d \geq 3 \text{ mm}) \quad (9)$$

It must be appreciated that this formula should be applied for rough approximative, comparative purposes only. It is developed not for the purpose of predicting absolute stress values, but to evaluate the qualitative effects of the most important frame parameters (7).

STRESS–RIGIDITY RELATIONSHIP

In the three formulas presented (Eqs. 5,7,9), the rigidity of the EFF frame (k_f), the maximal pin stress (σ_{sm}), and the peak pin–bone interface stress ($\bar{\sigma}_{bm}$) are related to the most significant frame parameters, such as the number of side bars (n_f) and the number of pins per fracture side (m), the side-bar separation (s), the pin diameter (d), and the pin modulus (E_s).

It is immediately obvious from the formulas that all parametric adaptions that increase the frame rigidity, reduce the pin and pin–bone interface stresses at the same time. This is illustrated in Fig. 3, where parametric effects on the frame flexibility ($1/k_f$) and the peak stresses are shown relative to the reference configuration. Evidently, the pin diameter is particularly effective in increasing frame rigidity and decreasing stresses, followed by the number of side bars. The number of pins has important effects on both the rigidity and the stresses, too. The side-bar separation and the pin modulus, however, affect the frame rigidity in particular, but the stresses to a lesser extent.

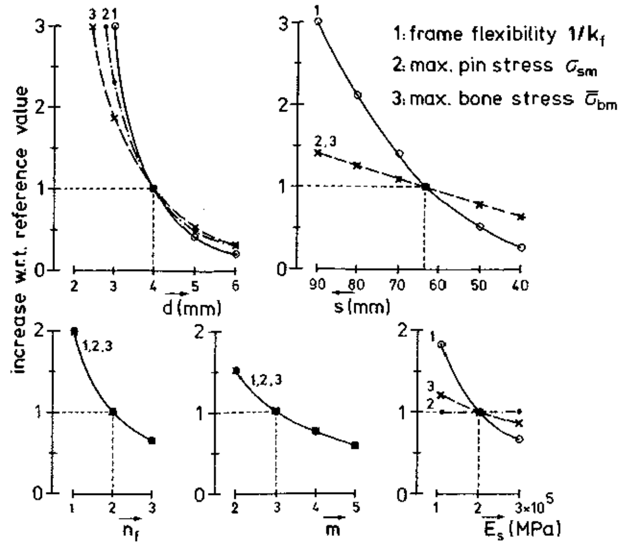

FIG. 3. Effects of the pin diameter (d), the side-bar separation (s), the number of side bars (n_f), the number of pins per side of the fracture (m), and the pin modulus (E_s) on the frame flexibility ($1/k_f$, the inverse of the frame rigidity), the maximal pin stresses, and the peak pin–bone stresses. It must be noted that in the case n_f = 1 (unilateral frame), the flexibility may be significantly higher in reality, due to side-bar bending.

These results give explicit guidelines in the case that the EFF frame rigidity must be maximized and stresses minimized. More importantly, however, they also provide useful guidelines when the frame must be flexible—hence, when a compromise between flexibility and acceptable stresses must be assessed. The most effective parameters to address in this case are the side-bar separation and the pin

2A,B

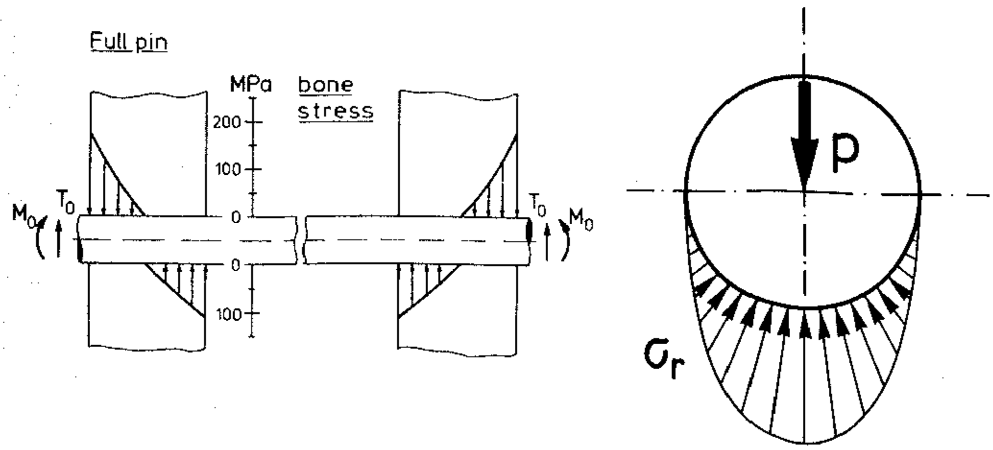

FIG. 2. Pin–bone interface compressive stress pattern in the case of a bilateral frame, shown along the pin (**A**) and in a cross section (**B**) (7).

modulus, because they have significant influences on the frame rigidity but only minor influences on the peak pin and pin–bone interface stresses (Fig. 3). For example, if the side-bar separation s is doubled, the frame flexibility increases eightfold, whereas the stresses increase only twofold. If the pins are made out of titanium, instead of steel, the frame flexibility is almost doubled, the pin stresses are not affected, and the pin–bone stresses increase only about 25%.

Whereas Fig. 3 gives information about the influences of separate parametric changes relative to the reference configuration, Fig. 4 puts all parametric combinations in perspective, in relation to pin stresses and frame rigidity. For given, arbitrary values of the pin diameter and modulus, the relative influences of the side-bar separation (s) and the product of numbers of side bars and pins ($n_f m$) on the frame rigidity and the pin stresses can be evaluated from Fig. 4A. The stress for $s = 40$ mm and $n_f m = 15$ (point σ_2) and the rigidity for $s = 90$ mm and $n_f m = 2$ (point k_1) are taken as base values in this nomogram. Hence, $\sigma_1 \approx 15\sigma_2$, and $k_2 \approx 80k_1$, according to the graph. Specific combinations of stresses and rigidity can be assessed from this graph. For example, the optimal compromise between stress magnitude and flexibility of the frame within the limits of the chosen parameter values is obviously found in the lower-left corner of the parallelogram ($s = 90$ mm and $n_f m = 15$), where $\sigma_{sm} \approx 2.1\sigma_2$ and $k_f \approx 7.5k_1$.

In the graph of Fig. 4A the pin diameter and modulus have arbitrary but constant values. For any given values of these parameters, rigidity and maximal pin stresses can be evaluated in an absolute sense as is illustrated in Fig. 4B. In this nomogram the maximal pin stresses per Newton force through the bone and the frame rigidity are related for pin diameters of 3, 4, 5, and 6 mm, assuming steel as the pin material. The relative parametric dependencies within each parallelogram of this graph can again be evaluated from Fig. 4A. Although this was not carried further, a comparable graph can be made for the case of titanium pins. However, it is believed that the information provided in the formulas and Fig. 3 is adequate to translate the graphs of Fig. 4 to the case of titanium pins. Because the pin modulus has no effect on the maximal pin stresses, the parallelograms in Fig. 4B only shift to the left when titanium is used.

An underlying assumption of the nomograms in Fig. 4 is that the flexibility of the side bars is negligible. This means that, in the case of a unilateral frame, the effects of side-bar bending must be added to the rigidity found from the nomogram, in accordance with Eq. 5A.

The peak pin–bone interface stresses are not taken into account in Fig. 4. However, Fig. 3 shows that their dependency on the frame parameters roughly follows the trends for the pin stresses.

Of note in Fig. 4 is the enormous range in which the EFF frame can be adapted within the limits of realistic parameter values. Comparing a configuration of three side bars and five pins ($n_f m = 15$), a pin diameter of 6 mm, and a side-bar separation of 40 mm on the one hand, with a configuration of one

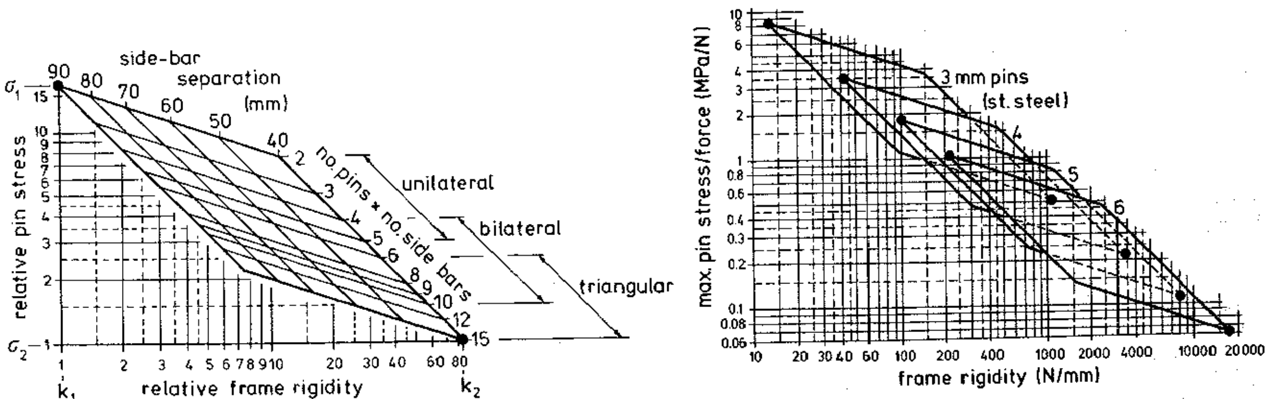

FIG. 4. Nomograms relating frame rigidity to maximal pin stresses, using the most important frame characteristics as parameters. **A**: For a given number of side bars x number of pins ($n_f m$) and side-bar separation (s), the relative rigidity (k_f/k_1) and the relative stress (σ_{sm}/σ_2) can be assessed. **B**: Then, using the given pin diameter, the actual rigidity (k_f) and the actual stress for unit applied force (σ_{sm}/F) can be evaluated. *Example:* $n_f = 2$ (bilateral frame), $m = 3$; hence, $n_f m = 6$; $s = 60$ mm. **A** gives $k_f \approx 10\, k_1$, $\sigma_{sm} \approx 3.8\, \sigma_2$. Assuming 5 mm pins, **B** gives $k_1 \approx 100$ N/mm and $\sigma_2 \approx 0.11$ MPa/N. Hence, $k_f \approx 1000$ N/mm and $\sigma_{sm} \approx 0.42$ MPa/N. Note that in the case $n_f = 1$ (unilateral frame), the rigidity may be significantly overestimated, as side-bar bending is neglected.

side bar, two pins ($n_f m = 2$), a pin diameter of 3 mm and a side-bar separation of 90 mm on the other hand, we have a range from about 0.06–8.3 MPa/N in the maximal pin stresses and a range from about 13 N/mm to 17,000 N/mm in the frame rigidity.

DISCUSSION AND CONCLUSIONS

It is obvious that the results presented here are based on rather simple analytical considerations. Hence, the models must be applied carefully and with understanding of the basic limitations. Although rather rough in absolute quantitative predictions, the formulas presented have the advantage of flexibility, simplicity, and easy applicability, and therefore give good insight into the significance of the most important parameters.

This paper suggests that the application of sophisticated and expensive numerical analysis methods such as the FEM is often unnecessary, because the relevant results can equally well be obtained with simpler and cheaper traditional methods of mechanics. Although this is sometimes true, one should not forget that, as in the present case, results from more complex theoretical and experimental models are often required as a reference data base.

The model presented here is limited to the axial loading case. In view of analytical considerations and FEM results (5), it may be anticipated that the frame parameters play the same role, qualitatively speaking, in bending and torsion. However, it is certain that the pin separation and the pin-group separation, which have no significant effect in the axial loading case, play an important role in bending and torsion (4,12). If such is deemed necessary, the present model could be expanded to take bending and torsion into account, using the same basic principles.

The models assume that the pins are well fixed to the bone and the side bars. In the case that loosening occurs, the frame rigidity will obviously be reduced. In addition, a fracture gap is assumed in the analysis. When fracture healing advances, the bone itself will contribute to the rigidity of the frame–bone structure. As a consequence, a part of the load will pass through the fracture and the frame load will decrease, resulting in accordingly decreased pin stresses and pin–bone interface stresses. Beaupré et al. (1) found in their "best estimate" FEM model, in the case that the bone completely healed, a rigidity of about 2,000 N/mm for the bone–frame configuration as a whole and a rigidity of about 80 N/mm for the frame alone. In this case, only 4% of the load should pass through the frame. As is evident from the nomogram in Fig. 4, however, this is not a general rule, in view of the wide range of frame rigidities possible. If, for instance, these authors had reduced the side-bar separation from 107 to 50 mm in their model, the frame rigidity would have increased 10-fold. In that case, about 30% of the load would pass through the frame in the extreme case of completely healed bone. Of course, the possibilities for reduction of the side-bar separation are limited, in view of the soft-tissue mantle.

In summary, it is suggested that the rigidity of an external fixation frame in axial loading (k_f), the maximal pin stresses (σ_{sm}), and the peak pin–bone interface stresses ($\bar{\sigma}_{bm}$) occurring when a fracture gap is present can be approximated by

$$k_f = 6\,\frac{n_f m E_s I}{s^3} \quad (n_f > 1)$$

$$k_f = \left(\frac{s^3}{6mE_sI} + \frac{s^2 l_p}{E_{sb} I_{sb}}\right)^{-1} \quad (n_f = 1)$$

$$\sigma_{sm} = \frac{sd}{4n_f m I}\,F$$

$$\bar{\sigma}_{bm} \approx sF\Big/\left[n_f m d\left(\frac{8E_sI}{LDk} + \frac{L^2}{3}\right)\right] \quad (d \geqslant 3 \text{ mm})$$

It is hoped that this model will find a use in EFF design and applications in clinical patient-evaluation studies and animal experiments. The nomograms of Fig. 4 can provide a quick reference to estimate stress and rigidity values in all cases.

REFERENCES

1. Beaupré GS, Hayes WC, Jofe MH, White AA: Monitoring fracture site properties with external fixation. *J Biomech Eng* 105:120–126, 1983
2. Briggs BT, Chao EYS: The mechanical performance of the standard Hoffmann-Vidal eternal fixation apparatus. *J Bone Joint Surg* 64A:566–573, 1982
3. Burny F: Elastic external fixation of tibial fractures, study of 1421 cases. In: *External Fixation, The Current State of the Art*, ed by AF Brooker Jr, CC Edwards. Baltimore, Williams & Wilkins, 1979
4. Chao EYS, An KN: Biomechanical analysis of external fixation devices for the treatment of open bone fracture. In:

Finite Elements in Biomechanics, ed by RH Gallagher, BR Simon, PC Johnson, JF Gross, New York, Wiley, 1982

5. Chao EYS, Kasman RA, An KN: Rigidity and stress analysis of external fracture fixation devices—A theoretical approach. *J Biomech* 15:971–983, 1982
6. Hart MB, Wu JJ, Chao EY, Kelly PJ: External skeletal fixation of canine tibial osteotomies—Compression vs no compression. *J Bone Joint Surg* 67A:598–605, 1985
7. Huiskes R, Chao EYS, Crippen TE: Parametric analyses of pin–bone stresses in external fixation devices. *J Orthop Res* 3:341–349, 1985
8. Johnson HF, Stovall SC: External fixation of fractures. *J Bone Joint Surg* 32A:466, 1950
9. Johnson WD, Fisher DA: Skeletal stabilization with a multiplane external fixation device—Biomechanical evaluation and finite element model. *Clin Orthop* 180:34–43, 1983
10. Lewallen DG, Kasman RA, Chao EY, Kelly PJ: Comparison of the effects of compression plates and external fixators on early bone-healing. *J Bone Joint Surg* 66A:1084–1090, 1984
11. McCoy MT, Kasman RA, Chao EY: Comparison of mechanical performance in four types of external fixators. *Clin Orthop* 180:23–33, 1983
12. Tencer AF, Claudi B, Pearce S, Bucholz RW, Johnson KD: Development of a variable stiffness external fixation system for stabilization of segmental defects of the tibia. *J Orthop Res* 1:395–404, 1984
13. Vidal J: External fixation—Yesterday, today and tomorrow. *Clin Orthop Rel Res* 180:7–14, 1983
14. Vidal J, Buscayret C, Connes H, Puran M, Allieu Y: Traitement des fractures ouvertes de jambe par le fixateur externe en double cadre. *Rev Chir Orthop* 62:433, 1976
15. Wu JJ, Shyr HS, Chao EY, Kelly PJ: Comparison of bone fracture healing under external fixation with varying stiffness characteristics. *J Bone Joint Surg* 66A:1258–1264, 1984